

RESEARCH ARTICLE

Adsorption Equilibrium and Kinetic Characterization of Methylene Blue on Coffee Grounds Activated Carbon

Seung-Woo Lee¹, Tae-Young Kim¹, Seon - Gyun Rho²

¹Department of Environmental Energy Engineering, Chonnam National University, Gwangju 61186, Korea.

²Department of Fire Service Administration, Honam University, Gwangju 62399, Korea.

Received: 3 August 2025 Accepted: 19 August 2025 Published: 26 August 2025

Corresponding Author: Tae-Young Kim, Department of Environmental Energy Engineering, Chonnam National University, Gwangju 61186, Korea.

Abstract

The adsorption characteristics of methylene blue (MB) from aqueous solution on coffee grounds activated carbon (CGAC) were studied. The CGAC was characterized by BET, SEM, TGA and FT-IR techniques. The adsorption capacity of MB on CGAC was greater than that of coffee grounds. The adsorption equilibrium isotherms were well fitted with the Sips equation. The estimated values for the free energy of adsorption (ΔG°) were -2.90, -3.27, and -3.46 kJ/mol at 288, 298 and 308K, which indicated that a spontaneous process. Kinetic studies showed that the adsorption of MB on CGAC in the system followed pseudo-second-order kinetics.

Keywords: Adsorption, Coffee, Dye, Equilibrium, Kinetic.

1. Introduction

Urban and industrial activities commonly generate harmful components such as organic chemicals or heavy metals, that have a serious impact on the ecological systems and the food chain indefinitely [1-4]. Discharge of dyes from various industries into the environment and drinking water sources causes numerous health issues and significant harm, including skin sensitivity, carcinogenic effects, and mutagenic changes in living organisms [5,6]. The sectors producing the most dye wastewater include textiles, printing, paper, food processing, and tanneries. Approximately 200,000 tons of textile dyes are produced annually [7]. Among these dyes, methylene blue (MB) is a cationic dye and the most common colorants used as water-soluble organic dyes. MB is not extremely hazardous but inhalation causes rapid breathing, vomiting, shock, mental confusion, and nausea in humans [8,9]. Hence, it is important to remove MB and other dyes from water systems to reduce their impact on the environment.

Therefore, the development of novel materials or technologies to effectively remove these contaminants is highly desired. Among numerous methods have been developed to remove dyes from wastewater such as biodegradation, photocatalytic degradation, membrane separation. However, biological methods for MB removal are time-consuming, making them less efficient for industrial-scale applications involving high concentrations of dyes [10]. On the other hand, photocatalytic degradation has several drawbacks that limit its industrial-scale application, including low utilization of visible light, rapid charge recombination, and suboptimal electron and hole migration generated through photochemical processes [11]. Membrane technology for MB removal incurs high operational costs due to the high-cost membranes and the need for periodic replacement caused by fouling [12]. Adsorption processes have been found to be superior than other methods because of its attractive features such as high specific surface area, efficiency, and convenience in removing targets from aqueous solution [13-15]. There are many

Citation: Seung-Woo Lee, Tae-Young Kim, Seon - Gyun Rho. Adsorption Equilibrium and Kinetic Characterization of Methylene Blue on Coffee Grounds Activated Carbon. Open Access Journal of Chemistry. 2025;7(1): 81-90.

©The Author(s) 2025. This is an open access article distributed under the Creative Commons Attribution License, which permits unrestricted use, distribution, and reproduction in any medium, provided the original work is properly cited.

agricultural wastes used to manufacture activated carbon, which reduces the cost of raw material and protects the environment from pollution [16,17]. The raw materials commonly include seed of fruit, rice husk, bean shell, reed, corn cob, coffee waste and other renewable resources. Coffee is one of the most abundant agricultural products as well as the one of the major drinks in the world. The amount of coffee bean consumption in Korea was about 216,000 tons in 2024 and about 173,000 tons of coffee grounds are annually generated. However, most of them are simply landfilled or incinerated. Although there is still a shortage of coffee waste recycling technologies compared to the amount of coffee grounds produced.

The aims of present work were to prepare activated carbon from coffee grounds (CGAC) and characterized from N_2 adsorption/desorption isotherms, Fourier transform infrared spectroscopy (FT-IR), thermogravimetric analysis (TGA), scanning electron microscopy (SEM). CGAC was then utilized for MB removal under various operational conditions, such as the pH and temperature of the MB solution, CGAC mass, contact time. In addition, the adsorption equilibrium isotherm and kinetics for MB on CGAC were studied. The thermodynamic parameters were calculated using adsorption equilibrium isotherms.

2. Materials and Methods

2.1 Adsorbate

MB, a cationic pollutant in which the chemical formula of $C_{16}H_{18}N_3SCl \cdot 3H_2O$, molecular weight of 373.9 g/mol and λ max of 664 nm, was selected as the adsorbate in this research work. The stock solution was purchased from Aldrich Chemical. All other chemical reagents used were of analytical grade.

2.2 Preparation of Biochar

Coffee grounds were collected from local cafe (Gwangju, Koea). The samples were washed with hot distilled water to remove the brown color and residual organics and then dried at 100°C for 24 h. The particles were separated using the US standard testing sieve (No. 40-50) and immersed in 60wt% KOH solution for 24 h. The obtained material was placed in a furnace, followed by heating to the carbonization temperature 450°C at an increasing rate of 10°C/min and maintaining at the temperature for 0.5 h under N_2 flow protection. Activation temperature 750°C, and maintaining at the temperature for 3 h. The obtained CGAC was washed with deionized water until the pH of neutral. After dried the biosorbent, stored in a sealed

bottle with a silica gel to prevent the re-adsorption of moisture.

2.3 Equilibrium Studies

The MB was dissolved in deionized water to the required concentration (and then temperature of the dye solutions was adjusted to 288, 298, and 308K using a constant temperature water bath. Adsorption equilibrium isotherms were determined by bringing a known volume of the MB solutions (100 mL) into contact with carefully weighed amounts of the coffee ground and CGAC (0.01- 0.2g) in a conical flasks and then shaken for 24 h using a shaking incubator. The dye concentration of the solutions was analyzed at wavelength 664nm by an UV-VIS spectrometer (UV-2100PC, Shimadzu). The amount of adsorption of MB on CGAC at equilibrium q_e (mol/kg) was computed as follows.

$$q_e = \frac{(C_0 - C_e)V}{W} \quad (1)$$

where C_0 and C_e are the initial and equilibrium solution concentrations (mol/m³), respectively, V is the volume of the solutions (m³) and W is the weight of CGAC (kg).

2.4 Isotherm Modeling

Adsorption equilibrium isotherms are very important in describing the interactive behavior between adsorbate and biosorbent. The adsorption isotherm models of the Langmuir, Freundlich and Sips were fitted to describe the equilibrium adsorption of MB on CGAC. These isotherm equations are given below [18-20].

$$\text{Langmuir isotherm, } q = \frac{q_m k_L C_e}{1 + k_L C_e} \quad (2)$$

where k_L is the Langmuir affinity constant (m³/mol) and q_m is the maximum adsorption capacity of the material (mol/kg) assuming a monolayer of adsorbate taken up by the adsorbent.

$$\text{Freundlich isotherm, } q = k_F C_e^{1/n} \quad (3)$$

where k_F is the Freundlich constant related to the adsorption capacity (mol/kg)(mol/m³)^{-1/n} and n is the Freundlich exponent (dimensionless).

$$\text{Sips isotherm, } q = \frac{q_m k_s C_e^{1/n}}{1 + k_s C_e^{1/n}} \quad (4)$$

where k_s is the Sips constant related to the affinity constant (mol/m³)^{-1/n} and q_m is the Sips maximum adsorption capacity (mol/kg).

3. Results and Discussion

3.1 Characterization of Biosorbent

The specific surface area and pore size distribution of the CGAC used in this study were measured using N_2 adsorption /desorption isotherms at 77K (Fig. 1). The surface area, average pore diameter and total pore volume of the CGAC were $2,423\text{m}^2/\text{g}$, 18.91\AA and 1.15cc/g , respectively. In case of coffee ground, which were $35.4\text{m}^2/\text{g}$, 1.23\AA and 0.001cc/g ,

respectively. According to the International Union of Pure and Applied Chemistry (IUPAC) classifications, pores can be divided in broad terms according to their diameter (d) into macro pores ($d > 50\text{nm}$), meso pores ($2 < d < 50\text{nm}$) and micro pores ($d < 2\text{nm}$) [21]. Based on the results, it can be concluded that the pores of the CGAC fell into the category of micro pores. Surface morphology revealed important details regarding the surface structure of CGAC. As could be seen in Fig. 2

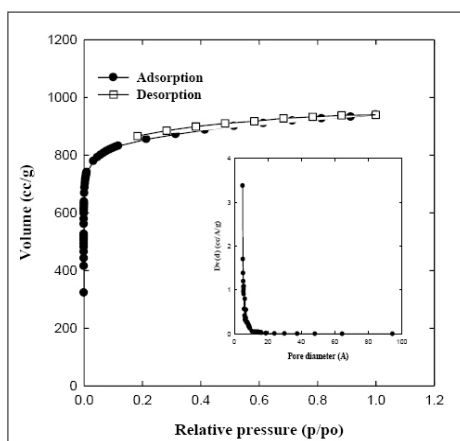


Figure 1. N_2 Adsorption/desorption isotherms and pore size distribution of CGAC at 77K.

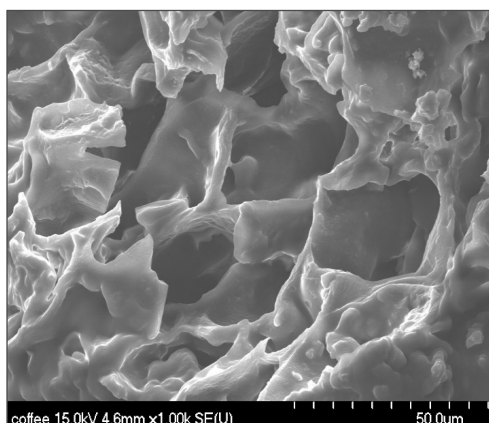


Figure 2. SEM image of CGAC.

Cylindrical pores of various shapes and sizes distributed all over the surface of CGAC. The CGAC sample shows an irregular surface structure, which might be due to the combination of chemical activation (KOH) and heat treatment. Fig. 3 presents the thermo-gravimetric analysis (TGA) curve and differential thermogram (DTG) of the sample acquired using a Perkin Elmer SII analyzer. During the analysis, 4.7 mg of the sample was heated up to 800°C at a heating rate of $10^\circ\text{C}/\text{min}$ under a nitrogen atmosphere. The decomposition process of the coffee grounds comprised two stages. Below the temperature of 220°C , the first stage of decomposition of coffee grounds corresponding to the loss of both the moisture and volatile matter. In the current study, the moisture and volatile matter content was recorded to

be 7.31%. The second stage of $220\text{--}500^\circ\text{C}$, in which accounts for more than 75.29% weight loss of coffee grounds according to polysaccharides decomposition. Ballesteros et al. showed that spent coffee grounds contain galactose, arabinose, glucose, mannose and other polysaccharides in various proportions [22]. In a temperature range of $220\text{--}500^\circ\text{C}$ with two peaks emerging at 290 and 345°C , respectively. The first peak is attributable to the decomposition of hemicellulose and the second to cellulose, both of which are the main components of coffee grounds.

FT-IR was used to analyze changes in the surface properties of the samples during the heat treatment process. The spectra are shown in Fig. 4. Both the coffee ground and CGAC samples show strong, broad bands at 3385cm^{-1} and 667cm^{-1} that correspond to the

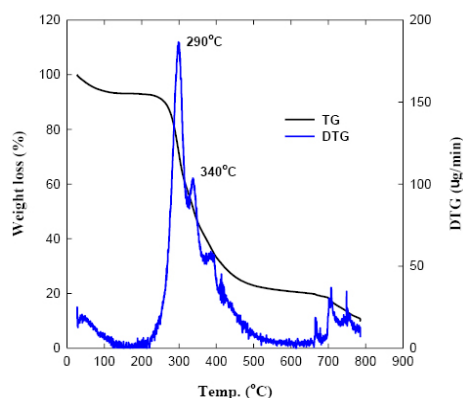


Figure 3. Thermo-gravimetric analysis of coffee grounds.

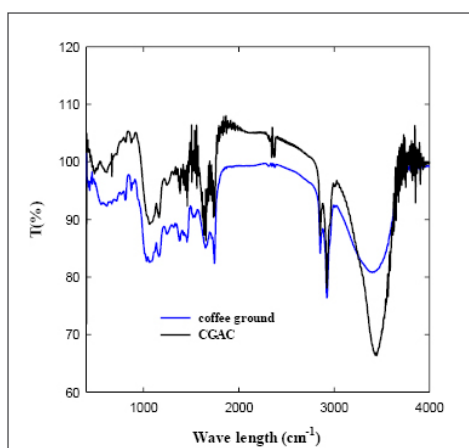


Figure 4. FT-IR spectra of coffee ground and CGAC.

-OH bond. According to Khalil et al. and Sain and Panthapulakkal, the cellulose component causes the -OH stretching vibration as the atoms are connected by intramolecular hydrogen bonds [23,24]. The peaks between 2854cm^{-1} and 2924cm^{-1} are related to the CH , CH_3 , and CH_2 bonds in aliphatic organic compounds, most of which were destroyed during the carbonization process [25]. The peaks between 1031cm^{-1} and 1165cm^{-1} are related to the C-O and C-O-C bonds in ether groups. In addition, the peaks between 812cm^{-1} and 869cm^{-1} are associated with C-O bonds [26]. After the carbonization process, all the peaks related to C-O and C-O-C bonds decreased.

3.2 Adsorption Isotherms

Adsorption is a surface phenomenon that can be defined as the increase in concentration of a particular component at the surface or interface between liquid and solid. Adsorption equilibrium isotherms for MB adsorption on CGAC as well as on coffee grounds at 298K are shown in Fig. 5. It is evident that the adsorption capacity of MB on CGAC (0.44mol/kg) is greater than that of coffee grounds (0.36mol/kg). The CGAC would be expected to increase the adsorption capacity of the dye ions, due to the surface area of CGAC ($2,423\text{m}^2/\text{g}$) higher than that of coffee grounds ($35.4\text{m}^2/\text{g}$). Fig. 6 shows that the adsorption capacity of

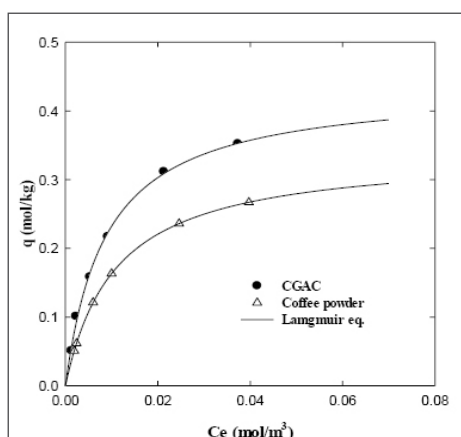


Figure 5. Adsorption equilibrium isotherms of MB on different adsorbents.

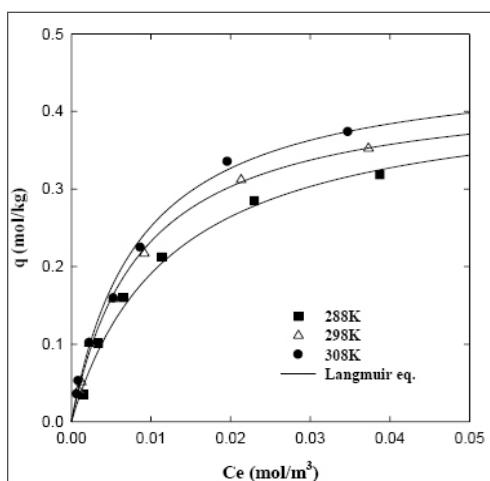


Figure 6 . Adsorption equilibrium isotherms of MB on CGAC at different temperature.

MB on CGAC increased with increasing temperature from 288 to 308K. The maximum amounts of MB adsorbed on CGAC at 288, 298, and 308K were 0.43, 0.44 and 0.47mol/kg. These phenomena may be caused that the dye molecular may penetrate faster and deeper at higher temperatures via swelling of the internal structure of the adsorbent. Jung et al. studied the adsorption of acid orange and methylene blue on spent coffee grounds and found that the adsorption increased with increasing temperature [27-29]. The Langmuir and Sips models imply that the solid surface is homogeneous and that only mono molecular layer adsorption occurs, while the Freundlich model suggests that dyes are adsorbed in a multi-layered manner in a heterogeneous medium. The Langmuir, Freundlich, and Sips models were employed and the determined isotherm model constants are summarized in Table 1. As shown in Table 1, the lowest error (%) values were estimated by the Langmuir isotherm equation. Generally, smaller error values reflect greater coherence between the model and experimental results. In this study,

three isotherm models, the Langmuir, Freundlich and Sips models, were used to correlate our experimental equilibrium data. The linear least square method and pattern search algorithm were used to identify the parameters for each adsorption isotherm. The value of the mean percentage error has been used as a criterion for testing the fit of the correlations. The mean percent deviation between the experimental and predicted values was obtained using Eq. (5).

$$error(\%) = \frac{100}{N} \sum_{k=1}^N \left[\frac{|q_{exp,k} - q_{cal,k}|}{q_{exp,k}} \right] \quad (5)$$

where $q_{cal,k}$ corresponds to the values of q predicted by the fitted model and $q_{exp,k}$ those measured experimentally. N is the number of experiments performed. The parameters and the average percent differences between measured and calculated values for MB on CGAC are given in Table 1. As shown in Table 1, the Langmuir model gives the best fit of our experimental data.

Table 1 . Adsorption equilibrium constants of MB on CGAC in terms of temperature.

Isotherm type	Parameters	Temperature (K)			
		288	298	298 Coffee ground	308
Langmuir	q_m	0.43	0.44	0.36	0.47
	b	79.96	114.39	81.42	117.56
	error(%)	8.66	4.22	3.35	5.59
Freundlich	k	3.30	2.52	1.76	3.41
	n	1.55	1.82	1.84	1.67
	error(%)	19.41	13.30	9.12	11.94
Sips	q_m	0.43	0.44	0.36	0.47
	b	96.93	112.27	82.78	105.68
	n	0.96	1.00	0.99	1.02
	error(%)	7.70	4.35	3.36	5.62

The adsorption amounts of MB on CGAC at different temperatures were used to obtain the thermodynamic parameters for the adsorption process. The thermodynamic parameters, i.e., the Gibbs free energy of adsorption (ΔG°), the enthalpy change (ΔH°) and the entropy change (ΔS°) have been estimated to evaluate the feasibility and exothermic nature of the adsorption process. In this research, thermodynamic parameters were calculated using the following equations.

$$\Delta G^\circ = -RT \ln K_s \quad (6)$$

$$\ln k_s = \frac{\Delta S^\circ}{R} - \frac{\Delta H^\circ}{RT} \quad (7)$$

$$k_s = \frac{q_m}{C_e} \frac{v_1}{v_2} \quad (8)$$

Where, R is the universal constant (8.314J/mol K), T and k_s are the absolute temperature (K) and thermodynamic equilibrium constant, respectively. v_1 is the activity coefficient of the adsorbed solute, and v_2 is the activity coefficient of the solute in equilibrium suspension. The ratio of activity coefficients was assumed to be uniform in the dilute range of the solution [26]. As the concentration of the MB approached zero, the activity coefficient approached unity and Eq. (8) became

$$\lim_{C_e \rightarrow 0} \frac{q_m}{C_e} = k_s \quad (9)$$

The values of k_s are obtained by plotting $\ln q_m/C_e$ vs. C_e and extrapolating to $C_e = 0$. The calculated values of k_s and the correlation coefficients are listed in Table 2. At temperatures of 288, 298 and 308K, the

Table 2. Thermodynamic parameters for MB on CGAC in terms of temperature.

Temperature [K]	K_s	R^2	ΔG° [kJ/mol]	ΔH° [kJ/mol]	ΔS° [J/mol K]	R^2
288	3.36	0.96	-2.90	3.79	22.88	0.93
298	3.74	0.95	-3.27			
308	3.86	0.93	-3.46			

values of the Gibbs free energy for MB on CGAC were -2.90, -3.27, and -3.46kJ/mol. The values are all negative, indicating that the adsorption process was spontaneous. Furthermore, the absolute value of ΔG° becomes larger with the increment of temperature. In other words, the higher the temperature, the stronger the driving force of adsorption. Therefore, the adsorption of MB on CGAC occurs more easily and is the most effective at high temperature [30].

The value of enthalpy and entropy can be calculated from the slope and intercept of the Van't Hoff plot (Eq. (7)) of $\ln k_s$ vs. $1/T$, respectively (Fig. 7), and the

results are summarized in Table 2. The ΔH° value of MB adsorption on CGAC was 3.79kJ/mol. The positive ΔH° for MB adsorption indicates that the adsorption process was an endothermic reaction [31]. The ΔS° value of MB adsorption was 22.88J/mol K. This positive ΔS° for MB adsorption suggests that MB adsorption on CGAC reduced the degrees of freedom of the adsorbent molecules, with entropy reducing during the adsorption process. The thermodynamic studies results suggest that MB adsorption by the CGAC in aqueous solution is a spontaneous process and endothermic adsorption.

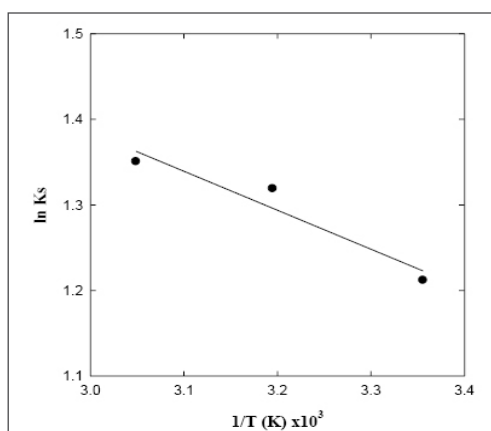


Figure 7. Plot of $\ln k_s$ vs. $1/T$ for the adsorptions of MB on CGAC.

3.3 Adsorption Kinetics

To measure the mass transfer mechanism of MB adsorption on CGAC in a batch system, using initial concentration decay curve. When the diffusion

resistance does not prevail, the transfer rate of any species to the external surface of the adsorbent, N_A , can be expressed by.

$$N_A = k_f A_s (C_o - C_e) \quad (10)$$

For a batch system with an adsorption time of less than 300 seconds, the following approximation holds.

$$\ln\left(\frac{C}{C_o}\right) = -k_f A_s t / V \quad (11)$$

In this equation, k_f and A_s are the film mass transfer coefficient (m/s) and the effective external surface

area of adsorbent particles (m^2), A_s , can be expressed as.

$$A_s = 3W / \rho_p R_p \quad (12)$$

Where, ρ_p and R_p are density and radius of CGAC, respectively. When $\ln(C/C_o)$ is plotted versus t of Eq. (11), a straight line with slope $-k_f A_s / V$ is obtained (Fig. 8). The values of calculated film mass transfer coefficient on CGAC of 0.1, 0.25, and 0.5g were 7.09×10^{-5} to 0.16×10^{-5} m/s.

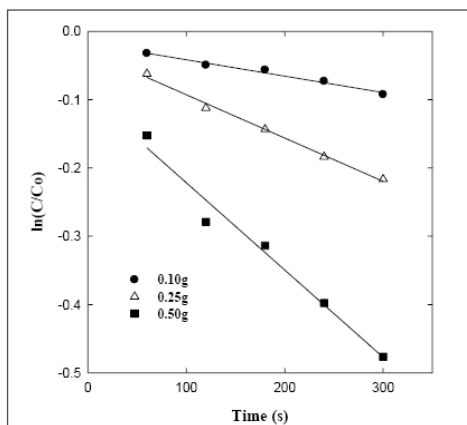


Figure 8. Determination of k_f from plots of $\ln(C/C_o)$ vs. time for MB on CGAC.

To measure order of reaction for the dye adsorption on CGAC, kinetic data were calculated by the pseudo-first-order and pseudo-second-order kinetic models [32]. The pseudo-first-order kinetic is presented as the following equation.

$$\log(q_{eq} - q_t) = \log q_{eq} - \frac{k_1}{2.303} t \quad (13)$$

where q_{eq} and q_t are the amounts (mol/kg) of adsorbed MB on CGAC at equilibrium and at time t , respectively, and k_1 is the rate constant ($1/\text{min}$). Fig. 9 shows the Lagergren pseudo-first-order kinetic plot for adsorption MB on CGAC in terms of dosage at 298K. The first-order rate constant, k_1 , and theoretical q_{eq} values were calculated from the slope

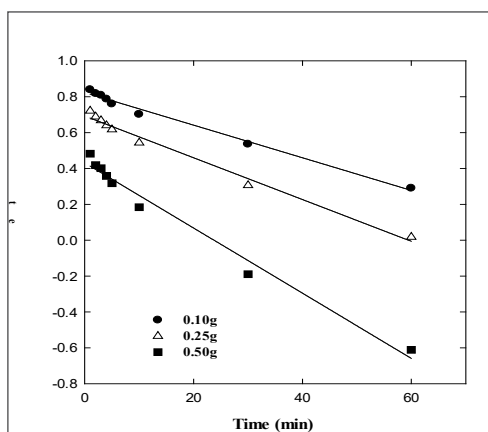


Figure 9. Linearized pseudo-first-order kinetic model in terms of dosage.

and intercept. The determined rate constants of k_1 , and theoretical q_{eq} values were in the range of 2.10×10^{-2} - $4.19 \times 10^{-2} \text{ min}^{-1}$ and 2.08×10^{-2} - $0.84 \times 10^{-2} \text{ mol/kg}$. The correlation coefficients (R^2) of the pseudo-first-order model for the linear plots of adsorption MB on CGAC are close to 1. Although the R^2 values can be reasonably high, the calculated q_{eq} values obtained from this kinetic model gave unreasonable values (Table 3), which were too low compared with those

obtained experimentally. This suggested that the adsorption process of MB on CGAC does not follow the Lagergren expression for pseudo-first-order adsorption. The sorption kinetics may be described by a pseudo-second-order model. The second-order kinetic model is expressed as.

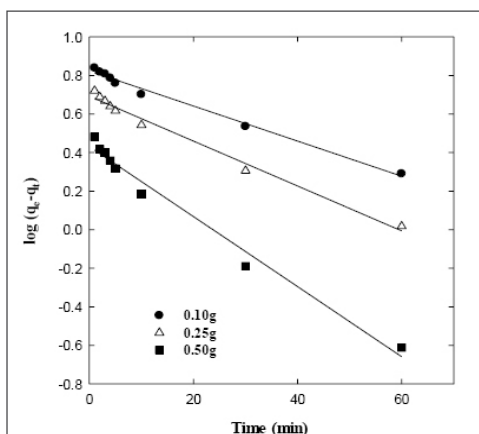
$$\frac{t}{q_t} = \frac{1}{k_{2,ad} q_{eq}^2} + \frac{1}{q_{eq}} t \quad (14)$$

Table 3. Kinetic parameters for MB on CGAC.

Dosage [g]	Pseudo-First Order			Pseudo-Second Order			Measured q_e $\times 10^2$ [mol/kg]
	$k_1 \times 10^{-2}$ [min ⁻¹]	$q_{eq} \times 10^{-2}$ [mol/kg]	R^2	$k_2 \times 10^{-2}$ [kg/mol min]	$q_{eq} \times 10^{-2}$ [mol/kg]	R^2	
0.10	2.10	2.08	0.99	0.60	2.61	0.97	2.36
0.25	2.67	1.54	0.99	1.05	1.97	0.99	1.80
0.50	4.19	0.84	0.98	3.64	1.19	0.99	1.13

where k_2 is the rate constant of the pseudo-second-order kinetic model (kg/mol min). The rate parameters k_2 and q_{eq} can be directly obtained from the intercept and slope of a plot of t/q_t versus t , as shown in Fig. 10. The values of k_2 and q_{eq} are shown in Table 3. The results in Table 3 show that the correlation coefficients (R^2) for the second-order kinetic model were close to

1. The values of k_2 increased with increasing dosage, presumably due to the enhanced mass transfer of the dye molecules to the surface of CGAC. The calculated equilibrium adsorption capacity (q_{eq}) is consistent with the experimental data. These results demonstrate that the pseudo-second-order adsorption mechanism is predominant.


Figure 10. Linearized pseudo-second-order kinetic model in terms of dosage.

4. Conclusion

The surface area, average pore diameter and total pore volume of the CGAC were 2,423m²/g, 18.91Å and 1.15cc/g, respectively. Adsorption amounts of MB on CGAC was greater than that of coffee grounds. The adsorption capacity of MB on CGAC increased with increasing temperature and the maximum adsorption amount was 0.47mol/kg (308K). The negative values of the Gibbs free energy for MB on CGAC indicated that a spontaneous process and the positive values of the enthalpy indicated that the adsorption process was an endothermic reaction. Film mass transfer coefficient of MB on CGAC calculated from concentration decay curves. Kinetic studies showed that the adsorption of MB on CGAC in the system followed pseudo-second-order kinetics.

Conflicts of Interest

The authors declare no conflicts of interest.

Funding

No funding was received for this manuscript.

5. References

1. Zhou W. Z., Chen J. A. S., Dai R.B., Wang Z. E., Selective removal of organic matters from high-salinity chemical industrial wastewater: Ultrafiltration or nanofiltration, *Water Research*, (2025) 282, 123762, <https://doi.org/10.1016/j.watres.2025.123762>.
2. Victor S. G. R., Beatriz E. B., Daniel C. G., Julian D. M. S., Henri S., Jules B. V. L., Degradation of p-cresol, resorcinol, and phenol in anaerobic membrane bioreactors under saline conditions, *Chemical Engineering Journal*, (2022) 430, 132672, <https://doi.org/10.1016/j.cej.2021.132672>.
3. Feng A., Jia Y. Z., Zhang K. T., Tian Z., Tian S. F., Wang X. K., Chi Y. Z., Fu S. L., Removal of organic pollutants from secondary treated effluent of a chemical industrial park using synchronized oxidation-adsorption (SOA), coagulation and Fenton processes: A comparison study, *Journal of Environmental Chemical Engineering*, (2025) 13, 117214, <https://doi.org/10.1016/j.jece.2025.117214>.
4. Anh H. D., Anh Q. H., An updated review on chemical compositions of cocoa products and by-products with

- a focus on toxic elements and organic pollutants, *Food Chemistry*, (2025) 489, 145001, <https://doi.org/10.1016/j.foodchem.2025.145001>.
5. Aravin P. P., A review of bioremediation of textile dye containing wastewater, *Cleaner Water*, (2025) 4, 100092, <https://doi.org/10.1016/j.clwat.2025.100092>.
6. Kayan G. O., Kayan A., Polyhedral Oligomeric Silsesquioxane and Polyorganosilicon Hybrid Materials and Their Usage in the Removal of Methylene Blue Dye, *Journal of Inorganic and Organometallic Polymers and Materials*, (2022) 32, 2781–2792, <https://doi.org/10.1007/s10904-022-02288-y>.
7. Solayman H. M., Hossen M. A., Abd Aziz A., Yahya N. Y., Leong K. H., Sim L. C., Monir M. U., Zoh K. D., Performance evaluation of dye wastewater treatment technologies: A review, *Journal of Environmental Chemical Engineering*, (2023) 11, 109610, <https://doi.org/10.1016/j.jece.2023.109610>.
8. Zanotti A., Baldino, L., Iervolino G., Cardea, D., Reverchon E., Chitosan aerogel beads production by supercritical gel drying, and their application to methylene blue adsorption, *The Journal of Supercritical Fluids* (2025) 226 106731, <https://doi.org/10.1016/j.supflu.2025.106731>.
9. Chiang C. H., Chen J., Lin J. H., Preparation of pore size tunable activated carbon derived from waste coffee grounds for high adsorption capacities of organic dyes, *Journal of Environmental Chemical Engineering*, (2020) 8, 103929, <https://doi.org/10.1016/j.jece.2020.103929>.
10. Saeed M., Muneer M., Haq A ul., Akram N., Photocatalysis: an effective tool for photodegradation of dyes—a review, *Environmental Science and Pollution Research*, (2022) 29, 293–311, <https://doi.org/10.1007/s11356-021-16389-7>.
11. Koe W. S., Lee J. W., Chong W. C., Pang Y. L., Sim L. C., An overview of photocatalytic degradation: Photocatalysts, mechanisms, and development of photocatalytic membrane, *Environmental Science and Pollution Research*, (2020) 27, 2522–2565, <https://doi.org/10.1007/s11356-019-07193-5>.
12. Oladoye P. O., Ajiboye T. O., Omotola E. O., Oyewola O. J., Methylene Blue Dye: Toxicity and Potential Elimination Technology from Wastewater, *Results in Engineering*, (2022) 16, 100678, <https://doi.org/10.1016/j.rineng.2022.100678>.
13. Demirci G. V., Baig M. T., Kayan A., UiO 66 MOF/Zr di terephthalate/cellulose hybrid composite synthesized via sol gel approach for the efficient removal of methylene blue dye, *International Journal of Biological Macromolecules*, (2024) 283, 137950, <https://doi.org/10.1016/j.ijbiomac.2024.137950>.
14. Ballesteros L. F., Cerqueira M. A., Teixeira J. A., Mussatto S. I., Characterization of polysaccharides extracted from spent coffee grounds by alkali pretreatment, *Carbohydrate Polymers*, (2015) 127, 347–354, <https://doi.org/10.1016/j.carbpol.2015.03.047>.
15. Khalil H. P. S. A., Ismail H., Rozman H. D., Ahmad M. N., The Effect of Acetylation on Interfacial Shear Strength between Plant Fibres and Various Matrices, *European Polymer Journal*, (2001) 37, 1037–1045, [https://doi.org/10.1016/S0014-3057\(00\)00199-3](https://doi.org/10.1016/S0014-3057(00)00199-3).
16. Sain M., Panthapulakkal S., Bioprocess Preparation of Wheat Straw Fibers and Their Characterization, *Industrial Crops and Products*, (2006) 23, 1–8, <https://doi.org/10.1016/j.indcrop.2005.01.006>.
17. Cao Y. H., Wang K. L., Wang X. M., Gu Z. R., Ambrico T., Gibbons W., Preparation of active carbons from corn stalk for butanol vapor adsorption, *Journal of Energy Chemistry*, (2017) 26, 35–41, <https://doi.org/10.1016/j.jechem.2016.08.009>.
18. Benjelloun, M., Miyah Y., Evrendilek G. A., Zerrouq F., Lairini S., Recent advances in adsorption kinetic models: their application to dye types, *Arabian Journal of Chemistry*, (2021) 14, 103031, <https://doi.org/10.1016/j.arabjc.2021.103031>.
19. Chu K. H., Debord J., Harel M., Bollinger J. C., Mirror, mirror on the wall, which is the fairest of them all? comparing the Hill, Sips, Koble–Corrigan, and Liu adsorption isotherms, *Industrial & Engineering Chemistry Research*, (2022) 19, <https://doi.org/10.1021/acs.iecr.2c00507>.
20. Rodríguez A., Ovejero G., Mestanza M., García J., Removal of Dyes from Wastewaters by Adsorption on Sepiolite and Pansil, *Industrial & Engineering Chemistry Research*, (2010) 49, 3207–3216, <https://doi.org/10.1021/ie9017435>.
21. Sing, K. S. W., Everett D. H. Haul, R. A. W., Reporting physisorption data for gas/solid systems with special reference to the determination of surface area and porosity. *Pure Appl. Chem.* (1985) 57, 603–619.
22. Ballesteros L. F., Cerqueira M. A., Teixeira J. A., Mussatto S. I., Characterization of polysaccharides extracted from spent coffee grounds by alkali pretreatment, *Carbohydrate Polymers*, (2015) 127, 347–354, <https://doi.org/10.1016/j.carbpol.2015.03.047>.
23. Khalil H. P. S. A., Ismail H., Rozman H. D., Ahmad M. N., The effect of acetylation on interfacial shear strength between plant fibres and various matrices, *European Polymer Journal*, (2001) 37, 1037–1045, [https://doi.org/10.1016/S0014-3057\(00\)00199-3](https://doi.org/10.1016/S0014-3057(00)00199-3).

24. Sain M., Panthapulakkal S., Bioprocess preparation of wheat straw fibers and their characterization, *Industrial Crops and Products*, (2006) 23, 1–8, <https://doi.org/10.1016/j.indcrop.2005.01.006>.
25. Li S. J., Han K. H., Li J. X., Li M., Lu C. M., Preparation and characterization of superactivated carbon produced from gulfweed by KOH activation, *Microporous and Mesoporous Materials*, (2017) 243, 291–300, <https://doi.org/10.1016/j.micromeso.2017.02.052>.
26. Gupta V. K., Singh P., Rahman N., Adsorption behavior of Hg(II), Pb(II), and Cd(II) from aqueous solution on Duolite C 433: a synthetic resin, *Journal of Colloid and Interface Science*, (2004) 275, 398–402, <https://doi.org/10.1016/j.jcis.2004.02.046>.
27. Jung K. W., Choi B. H., Hwang M. J., Jeong T. U., Ahn K. H., Fabrication of granular activated carbons derived from spent coffee grounds by entrapment in calcium alginate beads for adsorption of acid orange 7 and methylene blue, *Bioresource Technology*, (2016) 219, 185–195, <https://doi.org/10.1016/j.biortech.2016.07.098>.
28. Sabar S., Abdul Aziz H., Yusof N. H., Subramaniam S. Foo K. Y., Wilson L. D., Lee H. K., Preparation of sulfonated chitosan for enhanced adsorption of methylene blue from aqueous solution, *Reactive and Functional Polymers*, (2020) 151, 104584, <https://doi.org/10.1016/j.reactfunctpolym.2020.104584>.
29. Ahmad R., Ansari K., Comparative study for adsorption of congo red and methylene blue dye on chitosan modified hybrid nanocomposite, *Process Biochemistry*, (2021) 108, 92–102, <https://doi.org/10.1016/j.procbio.2021.05.013>.
30. Wang S. S., Li W. S., Li G. F., Polyethyleneimine modified spent coffee grounds as a novel bio adsorbent for selective adsorption of anionic Congo red and cationic Methylene blue, *Desalination and Water Treatment*, (2023) 290, 147–161, <https://doi.org/10.5004/dwt.2023.29480>.
31. Chen T., Da T. X., Ma Y., Reasonable calculation of the thermodynamic parameters from adsorption equilibrium constant, *Journal of Molecular Liquids*, (2021) 322, 114980, <https://doi.org/10.1016/j.molliq.2020.114980>.
32. Li X., Shen H., Pan X., Zou Z., Zhang H., Wang Y., Kinetic study of the fluoride removal by gypsum using revised pseudo-second-order model: Insights on the surface adsorption and precipitation, *Surfaces and Interfaces*, (2025) 62, 106304, <https://doi.org/10.1016/j.surfin.2025.106304>.